Front. Med. 2023, 17(2): 339–351
https://doi.org/10.1007/s11684-022-0943-0

RESEARCH ARTICLE

Sodium butyrate activates HMGCS2 to promote ketone body production through SIRT5-mediated desuccinylation

Yanhong Xu[1,*], Xiaotong Ye[2,*], Yang Zhou[2], Xinyu Cao[3], Shiqiao Peng[3], Yue Peng[4], Xiaoying Zhang[5], Yili Sun[6], Haowen Jiang[6], Wenying Huang[4], Hongkai Lian[5], Jiajun Yang[1], Jia Li[6], Jianping Ye (✉)[5,7]

[1]Neurology Department, Shanghai Jiao Tong University Affiliated Sixth People's Hospital, Shanghai 201306, China; [2]National Demonstration Center for Experimental Fisheries Science Education, Shanghai Ocean University, Shanghai 201306, China; [3]Shanghai Diabetes Institute, Shanghai Jiao Tong University Affiliated Sixth People's Hospital, Shanghai 200233, China; [4]School of Physical Education, Jiangxi Normal University, Nanchang 330022, China; [5]Metabolic Disease Research Center, Zhengzhou University Affiliated Zhengzhou Central Hospital, Zhengzhou 450007, China; [6]State Key Laboratory of Drug Research, Shanghai Institute of Materia Medica, Chinese Academy of Sciences, Shanghai 201203, China; [7]Center for Advanced Medicine, College of Medicine, Zhengzhou University, Zhengzhou 450007, China

Abstract **Ketone bodies have beneficial metabolic activities, and the induction of plasma ketone bodies is a health promotion strategy. Dietary supplementation of sodium butyrate (SB) is an effective approach in the induction of plasma ketone bodies. However, the cellular and molecular mechanisms are unknown. In this study, SB was found to enhance the catalytic activity of 3-hydroxy-3-methylglutaryl-CoA synthase 2 (HMGCS2), a rate-limiting enzyme in ketogenesis, to promote ketone body production in hepatocytes. SB administrated by gavage or intraperitoneal injection significantly induced blood β-hydroxybutyrate (BHB) in mice. BHB production was induced in the primary hepatocytes by SB. Protein succinylation was altered by SB in the liver tissues with down-regulation in 58 proteins and up-regulation in 26 proteins in the proteomics analysis. However, the alteration was mostly observed in mitochondrial proteins with 41% down- and 65% up-regulation, respectively. Succinylation status of HMGCS2 protein was altered by a reduction at two sites (K221 and K358) without a change in the protein level. The SB effect was significantly reduced by a SIRT5 inhibitor and in Sirt5-KO mice. The data suggests that SB activated HMGCS2 through SIRT5-mediated desuccinylation for ketone body production by the liver. The effect was not associated with an elevation in NAD^+/NADH ratio according to our metabolomics analysis. The data provide a novel molecular mechanism for SB activity in the induction of ketone body production.**

Keywords sodium butyrate; succinylation; HMGCS2; ketogenesis; SIRT5

Introduction

Ketone bodies are derivatives of long-chain fatty acids following the partial degradation in the liver and are used to fuel tissues, including brain and skeletal muscles. Ketone production is inhibited by insulin and induced by stress hormones through the regulation of free fatty acid levels in the blood. Lack of insulin in diabetes is a common cause of ketone body over production in ketoacidosis, a most common acute emergency in patients with diabetes mellitus [1]. Long-term fasting is another cause of ketoacidosis from a high level of lipolysis under starvation-induced energy crisis. However, in recent years, increasing studies have confirmed the beneficial metabolic activities of ketone bodies in the studies of aging, heart disease, epilepsy, and neurodegenerative diseases [2–5]. Ketosis is induced for disease treatment in some cases, and the induction is usually achieved by ketogenic diets with a very high fat ratio [6]. However, the exact mechanism of ketone diet action remains to be investigated.

Butyrate is a short chain fatty acid with four carbon atoms on the skeleton. It is one of the fermentation products of intestinal microflora. Butyrate is considered a signaling molecule for the gut microbiota in regulation of host metabolism. It improves insulin sensitivity, increases

Received February 27, 2022; accepted June 6, 2022

Correspondence: Jianping Ye, yejianping@zzu.edu.cn

*These authors contributed equally to this work.

energy expenditure in mice, and alleviates diet-induced obesity [7]. Butyrate regulates liver mitochondria in terms of function, efficiency, and dynamic in the study of insulin resistance in obese mice [8]. Butyrate may improve inflammatory bowel diseases, intestinal cancer, and neurodegenerative diseases [9–11]. Furthermore, it increases the plasma β-hydroxybutyrate (BHB) in animals [12,13] thus to be considered a potential substitute for ketogenic diet [6]. Butyrate has an advantage of low toxicity [14]. However, the molecular mechanism of ketogenic effect remains unclear for butyrate.

Butyrate increases protein acetylation by inhibition of histone deacetylase (HDAC). Post-translational modification (PTM) is an important mechanism in the regulation of protein functions, including phosphorylation, methylation, SUMOylation, acetylation, succinylation, and malonylation. PTM may regulate protein function quickly. In the nucleus, gene transcription is regulated by histone PTM, such as acetylation or methylation [15]. Butyrate is a classical histone deacetylase inhibitor, which induces histone hyperacetylation in favor of transcription initiation [16]. Butyrate also regulates PTM in cytoplasmic proteins, especially in mitochondrial proteins [17,18]. However, no report is available about SB activity in the regulation of protein succinylation in mitochondrial proteins.

In this study, we explored the mechanism of SB activity in the induction of ketogenesis in mice. In addition to acetylation, protein succinylation pattern was altered in the mouse liver detected by a targeted-proteomics approach. The SB activity was investigated using other approaches, such as targeted metabolomics, and Sirt5-KO mice.

Materials and methods

Animals and SB treatment

Male C57BL/6 mice were purchased from Gempharmatech Co., Ltd. (Nanjing, China) and maintained in the animal facility (SPF) of the Shanghai Sixth People's Hospital, Shanghai Jiao Tong University, with 12-h light–dark cycle, temperature of 22 °C ± 2 °C, humidity of 60% ± 5%, and free access to water and Chow diet (13.5% calorie in fat; Shanghai Slac Laboratory Animal Co., China). SIRT5-KO mice (Sv129) were a gift from Professor David Lombard of the University of Michigan. In the SB treatment, the mice were fasted for 8 h and then administrated with SB (S817488,MACKLIN, Shanghai, China) by intraperitoneal injection or gavage at dosages as indicated. The control mice were injected or fed with the same volume of saline. All animal procedures were conducted according to the animal protocol approved by the Institutional Animal Care and Use Committees (IACUC) at the Shanghai Sixth People's Hospital, Shanghai Jiao Tong University.

Targeted proteomics

For the targeted proteomics, 9 mice (C57BL/6) were used in each group. Mice were sacrificed at 0.5 h after SB intraperitoneal injection at the dose of 2.5 g/kg. Liver tissues were obtained immediately, frozen in liquid nitrogen, and kept in −80 °C refrigerator until proteomics was detected. Three liver tissues were pooled as one sample for the detection. Three samples in each group were analyzed by proteomics in protein modification for succinylation and acetylation.

Protein extraction

The samples were ground into powder after being frozen in liquid nitrogen and then transferred to a 5 mL centrifuge tube. Next, four volumes of lysis buffer (8 mol/L urea, 1% Protease Inhibitor Cocktail, 3 μmol/L TSA, 50 mmol/L NAM) were added to the cell powder, followed by sonication on ice using a high intensity ultrasonic processor for three times (Scientz, Ningbo, China). The remaining debris was removed by centrifugation at 12 000× *g* at 4 °C for 10 min. Finally, the supernatant was collected, and the protein concentration was determined using BCA kit (P0012, Beyotime, Shanghai, China).

Trypsin digestion

For digestion, the protein solution was reduced with 5 mmol/L dithiothreitol for 30 min at 56 °C and alkylated with 11 mmol/L iodoacetamide for 15 min at room temperature in darkness. Subsequently, the protein sample was diluted by adding 100 mmol/L TEAB to the urea concentration of less than 2 mol/L. Finally, trypsin was added at 1:50 trypsin-to-protein mass ratio for the first digestion overnight and 1:100 trypsin-to-protein mass ratio for a second 4 h-digestion.

Affinity enrichment

To enrich modified peptides, tryptic peptides dissolved in IP buffer (100 mmol/L NaCl, 1 mmol/L EDTA, 50 mmol/L Tris-HCl, 0.5% NP-40, pH 8.0) were incubated with pre-washed anti-succinylation beads (PTM-402, Jingjie PTM Biolabs, Hangzhou, China) or anti-acetylation beads (PTM-104, Jingjie PTM Biolabs, Hangzhou, China) at 4 °C overnight with gentle shaking. Then the beads were washed four times with IP buffer and twice with ddH_2O. The bound peptides were eluted from the beads with 0.1% trifluoroacetic acid. Finally, the eluted fractions were combined and vacuum-dried. For

LC-MS/MS analysis, the resulting peptides were desalted with C18 ZipTips (Millipore, Massachusetts, USA) according to the manufacturer's instructions.

LC-MS/MS analysis

The tryptic peptides were dissolved in 0.1% formic acid (solvent A). The gradient comprised an increase from 6% to 22% solvent B (0.1% formic acid in 98% acetonitrile) over 44 min, 22% to 30% in 12 min, and climbing to 80% in 2 min then holding at 80% for 2 min, all at a constant flow rate of 300 nL/min on an NanoElute UPLC system (Bruker Daltonics, Billerica, USA)

The peptides were subjected to capillary source followed by tandem mass spectrometry (MS/MS) in times-TOF Pro (Bruker Daltonics) coupled online to the UPLC. The applied electrospray voltage was 1.4 kV. Intact peptides and fragments were all detected and analyzed in the TOF system. The m/z scan range for full scan was 100 to 1700. The data acquisition mode was parallel accumulation-serial fragmentation (PASEF). The secondary spectrum was collected with 10 PASEF scanning after the primary spectrum was collected. The dynamic exclusion time was set to 24 s to avoid repeated scanning.

Database search

The MS/MS data were processed using Maxquant search engine (v.1.6.6.0). Tandem mass spectra were searched against SwissProt Mouse database concatenated with reverse decoy database. Trypsin/P was specified as cleavage enzyme that allows up to four missing cleavages. The mass tolerance for precursor ions was set as 40 ppm in the First search and 40 ppm in the Main search, and the mass tolerance for fragment ions was set as 0.04 Da. Carbamidomethyl on Cys was specified as fixed modification, and oxidation on Met, acetylation on protein N-terminal and succinylation on lysine were specified as variable modifications. False discovery rate (FDR) was adjusted to < 1%.

Bioinformatics methods

The subcellular localization was predicted using WoLF PSORT subcellular localization prediction soft. Soft MoMo (motif-x algorithm) was used in motif analysis. Proteins were classified by gene ontology (GO) annotation into three categories, namely, biological process, cellular compartment, and molecular function. Encyclopedia of Genes and Genomes (KEGG) database was used to identify enriched pathways to test the enrichment of the differentially modified protein against all identified proteins. For each protein category, InterPro database was researched to test the enrichment of the differentially modified protein against all identified proteins.

Primary hepatocytes culture

The primary hepatocytes were prepared and cultured according to a protocol in our published study [19]. 12–14-week-old male mice (C57BL/6 or Sv129 WT/Sirt5-KO) were anesthetized with 1% pentobarbital, then their abdominal cavities were opened under sterile conditions. Puncture was performed from the inferior vena cava using an indwelling needle, and the liver was perfused with the pre-perfusion fluid at 50 mL/mouse. The perfusion fluid flowed out from the hepatic portal vein, which was cut open after being punctured. Subsequently, a post-perfusion solution of 37 °C containing type IV collagenase (C5138, Sigma, USA) was infused. The perfused liver was cut off using surgical scissor and then crushed in a fresh serum-free medium to obtain the hepatocyte suspension. The hepatocyte suspension was filtered with a 200-mesh screen and centrifuged at 500 rpm for 1 min. The cell pellet was suspended in the mixture of Percoll cell separation solution (17-0891-02, Biodee, Beijing, China), serum-free medium, and 10× PBS, and centrifuged at 700 rpm for 20 min to obtain the primary hepatocytes in the pellet. The pellet was suspended in 10 mL of low glucose DMEM medium (containing 10% FBS and 1% penicillin-streptomycin) and seeded in the six-well plate precoated with 0.1% collagen at a density of 7×10^5 per well. Next, it was cultured at 37 °C in a 5% CO_2 incubator overnight. The cells were cultured in fresh serum-free DMEM when treated with SB.

Detection of BHB

BHB is the main component of ketone bodies. Blood and urine BHB levels were detected with a blood ketone/glucose meter (FreeStyle Optium Neo, Abbott, Chicago, USA). Blood of caudal vein was used for BHB test in the gavage or intraperitoneal injection models. We collected urine in 4 h following SB gavage, recorded the volume of urine for calculating the total BHB excreted in urine. The cell supernatant was used to reflect the ketogenesis of primary hepatocytes.

BHB in liver tissue was detected through the GC/MS method or a fluorometric assay kit. Liver tissues were obtained immediately after mice were sacrificed 1 h after SB was injected with the dose of 2.5 g/kg, and immediately frozen in liquid nitrogen and kept at −80 °C until detection. The GC/MS method was derived from a published protocol [20]. Liver tissues were ground in liquid nitrogen and re-suspended in 1 mL cold (−40 °C) 50% aqueous methanol that contained 100 μmol/L

norvaline as an internal standard. Moreover, samples were frozen on dry ice for 30 min and then thawed on ice. The samples were added with 400 μL chloroform and vortexed for 30 s before 10 min of centrifugation at 14 000 rpm (4 °C), and the supernatant was transferred to a 1.5 mL tube for drying and then stored at −80 °C before analysis. Metabolites were derivatized for GC/MS analysis as follows. First, 70 μL of pyridine was added to the dried pellet and incubated for 20 min at 80 °C. After cooling, 30 μL of *N*-*tert*-butyldimethylsilyl-*N*-methyltrifluoroacetamide was added, and samples were re-incubated for 60 min at 80 °C before being centrifuged for 10 min at 14 000 rpm (4 °C). The supernatant was transferred to an autosampler vial for GC/MS analysis. A Shimadzu QP-2010 Ultra GC-MS (Kyoto, Japan) was programmed with an injection temperature of 250 °C injection and injected with 1 μL of sample. GC oven temperature started at 110 °C for 4 min, rising to 230 °C at 3 °C/min and to 280 °C at 20 °C/min with a final hold at this temperature for 2 min. GC flow rate with helium carrier gas was 50 cm/s. The GC column used was a 20 m × 0.25 mm × 0.25 mm Rxi-5ms. GC-MS interface temperature was 300 °C, and (electron impact) ion source temperature was set at 200 °C, with 70 V ionization voltage. The mass spectrometer was set to scan m/z range of 50–800, with 1 kV detector.

BHB in the liver tissue was detected with a BHB (Ketone Body) Fluorometric Assay Kit (700740, Cayman Chemical, Michigan, USA). The liver tissue (35 mg) was ground in 350 μL of cold assay buffer, and proteins were removed from the homogenate by adding the same volume of 1 mol/L MPA. The supernatant was collected into a new 1.5 mL tube after centrifuging for 5 min at 10 000× *g* (4 °C). Potassium carbonate was used to adjust pH to 8.5. After centrifuging for 5 min at 10 000× *g* (4 °C), the supernatant was tested for BHB according to the guidance of the assay kit. The reaction was conducted in 50 μL sample, 25 μL of BHB fluorometric cofactors, 10 μL of BHB developing enzyme, and 10 μL of fluorometric developer reagent. The reaction plate was sealed and incubated for 30 min at 37 °C, and fluorescence intensity was obtained at the excitation wavelength of 530–540 nm and emission wavelength of 585–595 nm with a fluorescence microplate reader (Spectra Max i3X, USA).

Detection of NAD^+ and NADH by LC/MS

Six mice in each group were analyzed for NAD^+ and NADH in liver using the targeted metabolomics approach. The test was conducted using the ultra-performance liquid chromatography (Agilent 1290 Infinity LC) coupled with triple quadrupole mass spectrometry (5500 QTRAP, AB SCIEX), as described in our previous study [14]. Fresh liver tissues were collected 30 min after SB injection (2.5 g/kg, i.p.), frozen in liquid nitrogen immediately, and kept at −80 °C until analysis. The liver tissue (about 100 mg) was homogenized in ultra-pure water, treated with a mixture of methanol and acetonitrile (1:1 v/v), and centrifuged at 14 000× *g* at 4 °C to remove protein after incubation at −20 °C for 1 h. The supernatant was dried in vacuum and was used for the detection of metabolites in a mixture solution of acetonitrile and water (1:1, v/v). The data were analyzed using Multiquant program against the standard compounds.

Western blot and immunoprecipitation

Protein concentration was quantified with a BCA kit (P0012, Beyotime). Protein levels were determined by Western blot according to a protocol described elsewhere [14]. The protein samples (30 μg/sample) were loaded in the SDS-PAGE gel. To study protein–protein interaction, immunoprecipitation was used with 500 μg protein/sample in 500 μL lysis buffer. A total of 20 μL protein A agarose (P2006, Beyotime, Shanghai, China) and 4 μg antibody were added in the lysate, and then the mixtures were rotated overnight at 4 °C. After incubation, the mixtures were centrifuged at 2500 rpm for 5 min, the experimenter resuspended the precipitate (beads) with 1 mL cold 0.1% NP-40 lysis buffer, repeated the above procedure for another four times to wash the beads, and then added 25 μL 2× SDS-PAGE loading buffer, boiled at 100 °C for 10 min. The primary antibodies to SIRT5 (ab259967), GAPDH (ab181602), β-tubulin (ab6046), and acetylated H3K27 (ab4729) were obtained from Abcam (Cambridge, MA, USA). The primary antibody to HMGCS2 (#20940) was purchased from the Cell Signaling Technology (Boston, USA). Antibody to succinyllysine (PTM-401) was from Jingjie PTM Biolabs (Hangzhou, China). The antibody for immunoprecipitation (IP) (M21008) that can avoid heavy or light chain contamination was purchased from Abmart (Shanghai, China). The signal was collected with a chemiluminescence gel imager (Amersham Imager 600, GE Healthcare, USA), and the images were quantified using ImageJ software.

Statistical analysis

The data were statistically analyzed using the one-way ANOVA or Student *t*-test. *In vitro*, all experiments were repeated at least three times with consistent results. The data are presented as mean ± SEM with a significance of $P < 0.05$. In the targeted proteomics study, the difference was considered significant when $P < 0.05$, and the fold changes were more than 1.2 (upregulated) or less than 1/1.2 (downregulated).

Results

Butyrate changes succinylation of mitochondrial proteins in liver

PTM is an important approach in the control of substrate metabolism. As a HDAC inhibitor, SB induces histone acetylation in the control of gene transcription. However, there was no published report about SB activity in the regulation of protein succinylation. To address this issue, targeted proteomics was used to detect protein succinylation in the liver tissue of mice 0.5 h after SB injection (2.5 g/kg). Succinylation was detected in nearly 1000 proteins (985) from 6698 peptides (Fig. 1A). The protein exhibited a diversity in the number of succinylated sites from 1 to 53 per protein (Fig. 1B). A protein with the most succinylation sites is carbamoyl phosphate synthetase 1. Succinylation was altered in 84 proteins with a reduction in 58 proteins at 67 sites and an increase in 26 proteins at 27 sites at a 1.2-fold threshold (Fig. 1 C and 1D). In these proteins, majority (41 in total) were mitochondrial proteins, in which 24 proteins were downregulated and 17 upregulated in succinylation at a ratio of 1.4:1 (Fig. 1E and 1F). If the alteration threshold was increased to 1.5-fold, the total protein numbers were reduced to 46 with 40 downregulated at 47 sites and 6 upregulated at 6 sites. The ratio of mitochondrial proteins in down- and upregulation was increased to 19:2 (Fig. S1A). If the threshold was 2.0 folds, the ratio was 10:1 (Fig. S1B). The data suggests that the succinylation of mitochondrial proteins was actively regulated by SB for downregulation. The fold changes were twofold and above as listed in Table 1. Activities of those proteins were identified in many pathways but were dominant in the posttranslational modification, energy production, and lipid metabolism pathways by the COG/KOG (Cluster of Orthologous Groups of proteins) category for protein functions (Fig. 1G). The result demonstrated that SB induced an alteration in protein succinylation in the liver tissues with a dominant impact in the mitochondrial proteins.

Table 1 List of mitochondrial proteins at twofold threshold in succinylation change

Downregulated proteins	Upregulated proteins
Dihydrolipoyl dehydrogenase	Pyruvate carboxylase
Malate dehydrogenase	
Hydroxymethylglutaryl-CoA lyase	
Hydroxymethylglutaryl-CoA synthase	
60 kDa heat shock protein	
3-ketoacyl-CoA thiolase	
Acyl-coenzyme A synthetase ACSM1	
Cytosol aminopeptidase	
Serine-tRNA ligase	
Methylglutaconyl-CoA hydratase	

SB decreases the succinylation of ketogenesis rate-limiting enzyme

The aforementioned results suggest that SB downregulated mitochondrial protein succinylation. The proteins related to the synthesis and breakdown of ketone bodies were identified in the altered mitochondrial proteins in the SB-treated mice in KEGG database (Fig. 2A). Two enzymes (e.g., HMGCS2 and HMGCL) exhibited a reduction in succinylation in the ketone body synthesis pathway. HMGCS2 is the rate-limiting enzyme for ketone biosynthesis, whose activity is regulated by succinylation [21]. In the proteomics assay, succinylation was identified at 11 lysine residues in the HMGCS2 protein (Fig. 2B). A significant reduction was found at two sites, K221 (88%) and K358 (69%) (Fig. 2B). A modest reduction was observed at K342. Interestingly, increased succinylation (by 22%) was noted at the K354 site. Acetylation was also examined in the current study for the HMGCS2 protein to understand the mechanism of succinylation alteration. The two types of modifications may happen at the same lysine residues for a possibility of competition. The decreased succinylation may be a consequence of increased acetylation at K221 and K358. To address this possibility, seven acetylation sites were identified in the HMGCS2 protein (Fig. 2C), in which six were also subject to modification by succinylation. The acetylation of K221 was detected but was not changed by SB (Fig. 2C). The acetylation at the other lysin sites (K358) was not detected. Acetylation at two non-succinylation sites (e.g., K243 and K310) was enhanced (Fig. 2C). The data suggest that SB induced succinylation alteration in HMGCS2 protein with a dominant effect on downregulation. The effect was unlikely a result of changes in the acetylation status because the succinylation alteration was independent of acetylation pattern in the HMGCS2 protein.

Sodium butyrate (SB) raises blood ketone bodies

Plasma ketone bodies in mice were increased by SB through gavage or intraperitoneal injection. Blood BHB was determined in the tail vein using a ketone meter. A significant increase in BHB was observed in the first 2 h after SB gavage (Fig. 3A). The BHB elevation remained until the 4th hour. The urine ketone body was determined for 4 h after gavage. An increase in concentration and total amount was also observed (Fig. 3B and 3C). In the intraperitoneal injection model, the BHB elevation remained more than 4 h (Fig. 3D). The BHB elevation was detected in the liver tissue at 1 h of SB injection by GC/MS, and the increase was approximately 18-fold

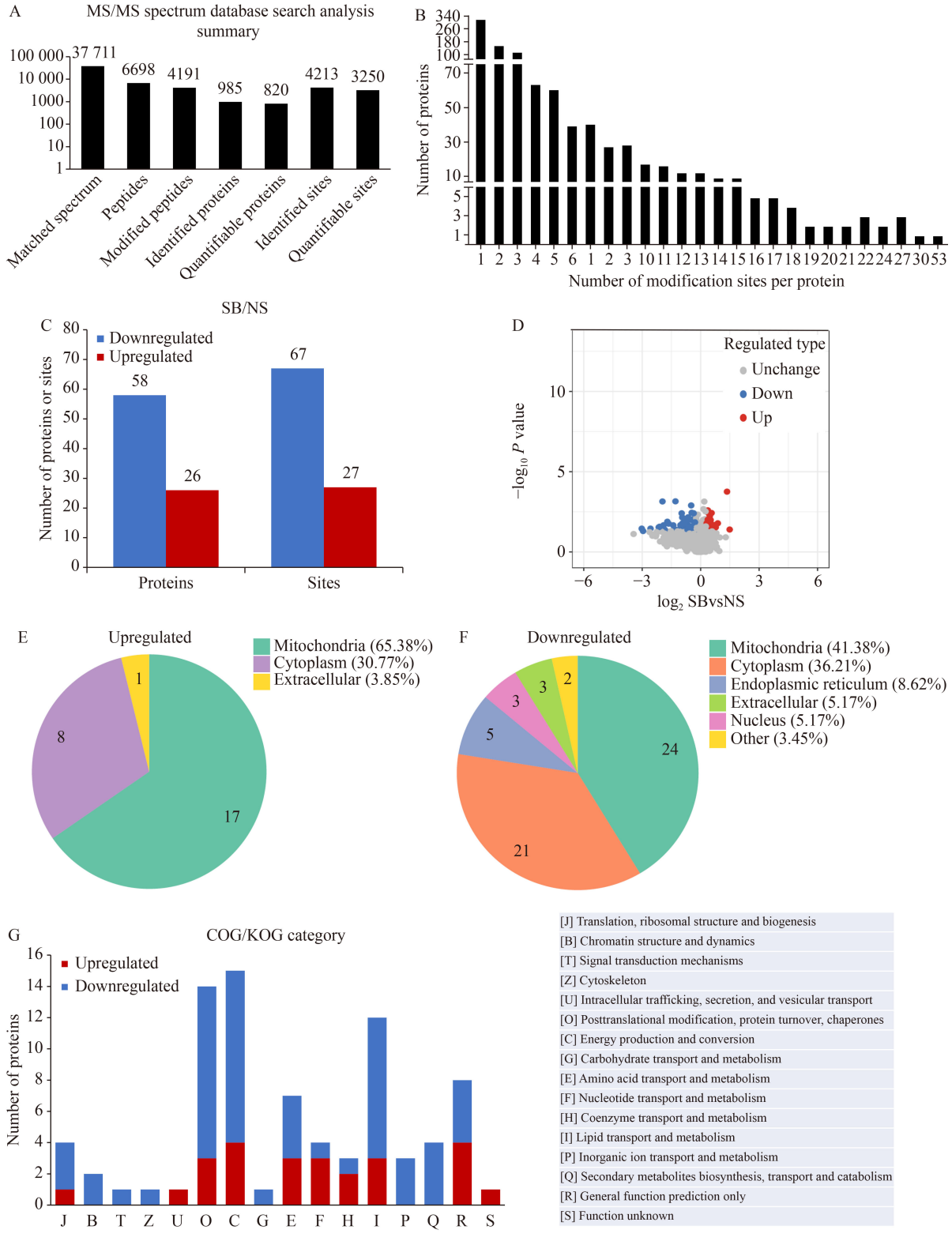

Fig. 1 General changes in protein succinylation status in mouse liver tissue. (A,B) General results of succinylation proteomics of liver tissue at 0.5 h after SB intraperitoneal injection (2.5 g/kg). (C,D) Succinylation profile of liver proteins after SB injection at 1.2-fold as threshold. NS, normal saline. (E,F) Subcellular locations of proteins with up- or downregulated succinylation. (G) Clusters of Orthologous Groups (COG) analysis of succinylation differential proteins. The livers of 3 mice were pooled to form one sample, and 3 samples were analyzed in each group in the proteomics study.

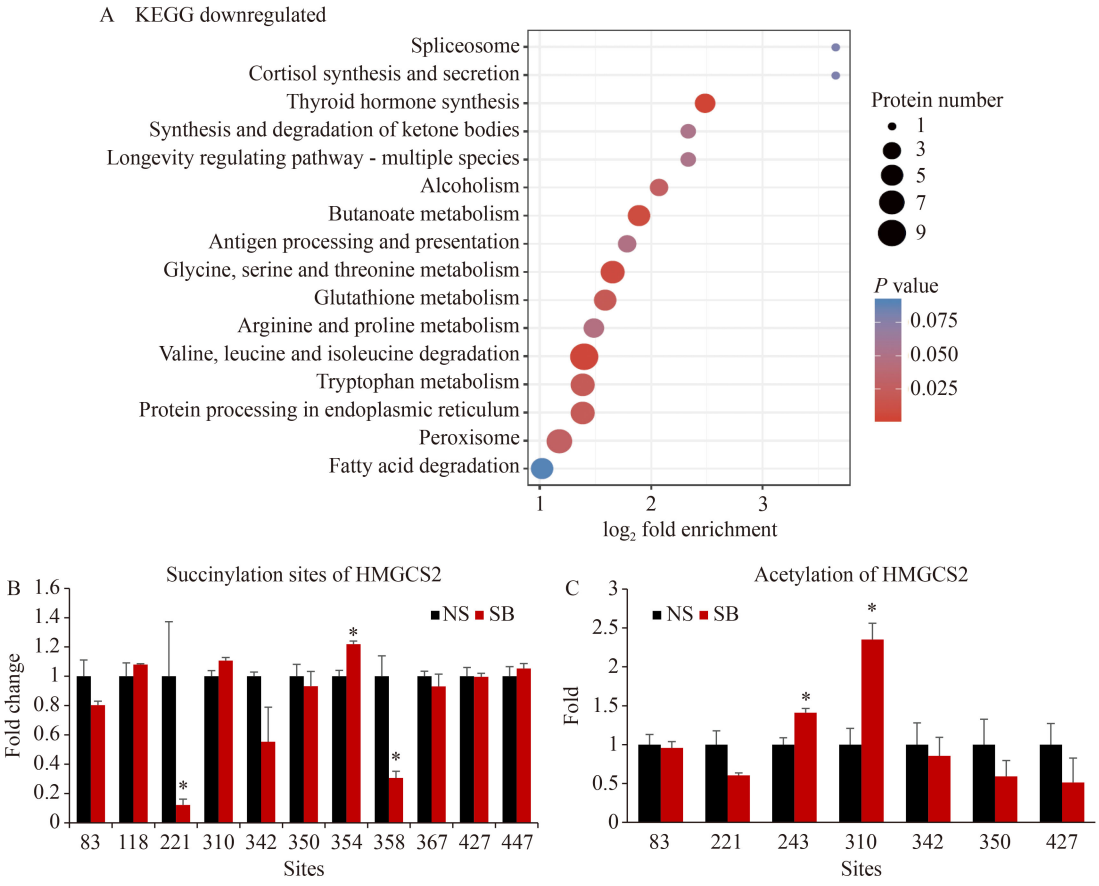

Fig. 2 Succinylation reduction in the key enzyme of ketogenesis pathway by SB treatment. (A) KEGG pathway from proteins with downregulated succinylation in the liver of SB-treated mice. (B) Succinylation status at different lysine residues in 3-hydroxy-3-methylglutaryl-CoA synthase 2 (HMGCS2). (C) Acetylation of HMGCS2 protein at lysin residues K243 and K310. * $P < 0.05$.

higher over the control mice (Fig. 3E). Absolute BHB concentration was detected at 74 nmol/100 mg wet liver tissue at 1 h of SB injection with a BHB fluorometric assay kit (Fig. 3F). The results suggest that SB induced BHB production in the liver and raised blood BHB regardless of the administration approach.

SB does not alter the protein abundance of HMGCS2 and SIRT5

The elevation of blood ketone body is usually a result of more production by the liver. As a rate-limiting enzyme in ketogenesis pathway, HMGCS2 was examined in protein abundance, and no change was observed in the liver of SB-treated mice (Fig. 4A–4D). The protein test was conducted at 5 time points (e.g., 10, 30, 60, 120, and 240 min) post SB injection. No significant change was detected in the liver tissue (Fig. 3C and 3D). A change in succinylation pattern was detected in the liver proteins using a pan-succinylation antibody in the whole cell lysate of liver tissue at 30 min of SB injection. Multiple bands of succinylation signals were observed in the assay, and a reduction was observed in bands 1, 2, and 3 in the SB-treated group (Fig. 4E and 4F). SIRT5, the only desuccinylase reported in the literature, was examined in the liver tissue. No change was observed in the protein abundance under the same condition (Fig. 4E and 4F). The results demonstrated that SB activity was associated with an alteration in the succinylation profile, but not with the protein abundance of HMGCS2.

SB elevates ketogenesis in hepatocytes

In the body, SB may induce ketone production through a direct or indirect effect on the liver. To test the direct effect, primary hepatocytes were prepared from mouse liver and treated with SB in the cell culture. BHB in the cell supernatant was determined to assess the SB effect. BHB was increased in the supernatant by SB in a time-dependent manner (Fig. 5A). At the same time, the succinylation was reduced in the cells by SB (Fig. 5B and 5C). The protein levels of HMGCS2 and SIRT5 were not changed in the cell model (Fig. 5D and 5E). In the control, the inhibitory activity of SB in HDACs was observed in the liver of SB-treated mice, in which the acetylation of histone protein was enhanced in a

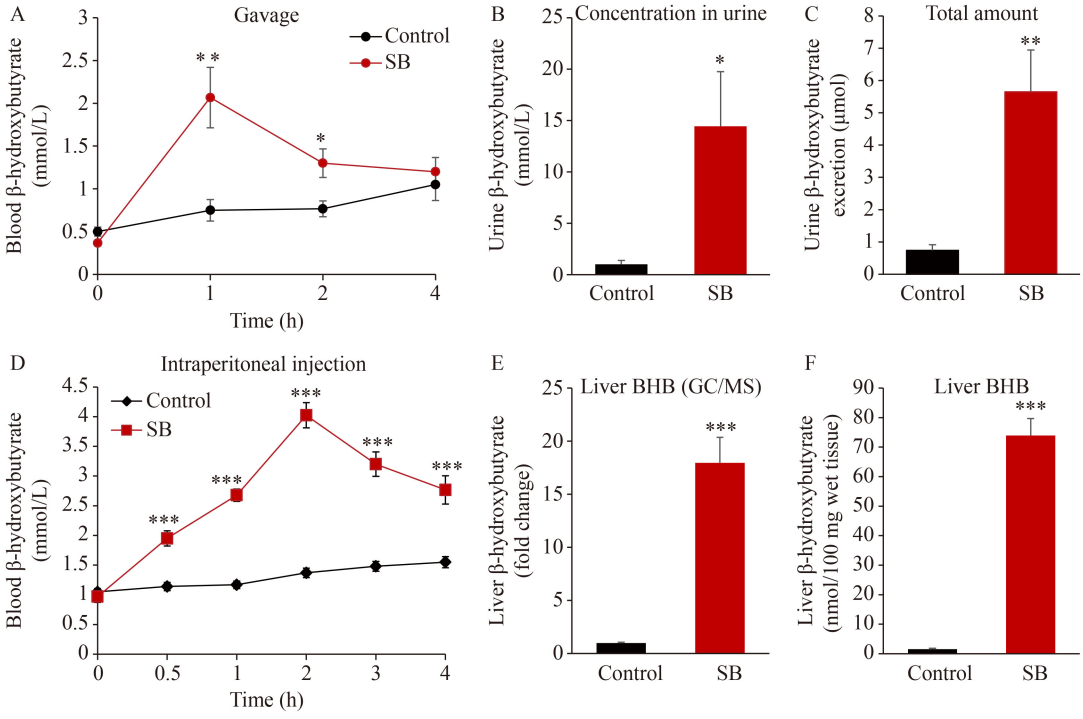

Fig. 3 SB induces ketogenesis. (A) Blood BHB levels in the gavage model (SB at 2.5 g/kg, $n = 6$). (B) BHB concentration in urine collected for 4 h after gavage ($n = 6$). (C) Total amount of BHB in the urine ($n = 6$). (D) Blood BHB levels in the intraperitoneal injection model (SB 2.5 g/kg, control $n = 10$; SB $n = 8$). BHB concentration was detected with a ketone meter. (E) Liver BHB levels determined by GC/MS method at 1 h of SB injection (2.5 g/kg, control $n = 9$; SB $n = 7$). (F) Liver BHB detected with the fluorometric assay kit. The assay was done in liver tissue at 1 h of SB (2.5 g/kg) injection ($n = 6$). * $P < 0.05$, ** $P < 0.01$, ***$P < 0.001$.

dose-dependent manner at H3K27, a well-established marker of acetylation (Fig. 5F). The data suggests that SB directly acted on hepatocytes to induce ketone body production in the liver by reducing the succinylation of HMGCS2 protein without changing the protein level.

SB increases HMGCS2/SIRT5 interaction

HMGCS2 activity is increased by desuccinylation that is catalyzed by SIRT5, whose enzyme activity is induced by an increased ratio of NAD^+/NADH [22]. A protein–protein interaction between HMGCS2 and SIRT5 is required for the desuccinylation. The above data suggest that SB may reduce succinylation through the induction of the protein interaction. To test the possibility, the interaction was examined in co-immunoprecipitation (Co-IP) in the liver tissue. The SIRT5 protein was pulled down using the HMGCS2 antibody (Fig. 6A and 6B), and SIRT5 protein was detected in the IP products. The SIRT5 signal was increased in the group of SB-treated mice. In the IP products of SIRT5 antibody, the HMGCS2 protein was detected, and the signal was enhanced in the SB-treated group (Fig. 6C and 6D). To understand the mechanism of SB activity in the interaction, NAD^+ and NADH levels were examined in the liver tissue using the metabolomics approach. The ratio of NAD^+/NADH was not altered in the SB-treated liver (Fig. 6E). These results suggest that the interaction of HMGCS2 and SIRT5 proteins was induced by SB in the liver, which was not associated with a change in NAD^+/NADH ratio.

SIRT5 mediates a part of the SB activity

The above data suggests that the SB effect may be dependent on SIRT5 in desuccinylation of HMGCS2. If this is true, then the inhibition of SIRT5 activity may cancel the SB effect. To test the possibility, SIRT5 was inhibited by a chemical inhibitor or gene knockout. In the primary hepatocytes, the SIRT5 activity was suppressed with the small molecule inhibitor MC3482 (HY-112587, MCE, USA), a specific inhibitor of SIRT5. The protein succinylation was increased in the treated cells, especially in bands 1 and 2 in WB (Fig. 7A and 7B). BHB level induced by SB was decreased by approximately 32% in the system (Fig. 7C). In the gene knockout system, Sirt5-KO mice were employed to test the SB activity (Fig. 7D). Succinylation was significantly increased in the liver proteins of the KO mice (Fig. 7E). The succinylation of HMGCS2 protein was increased in the same system without a change in the protein abundance (Fig. 7F and 7D). Ketone body production was decreased in the KO

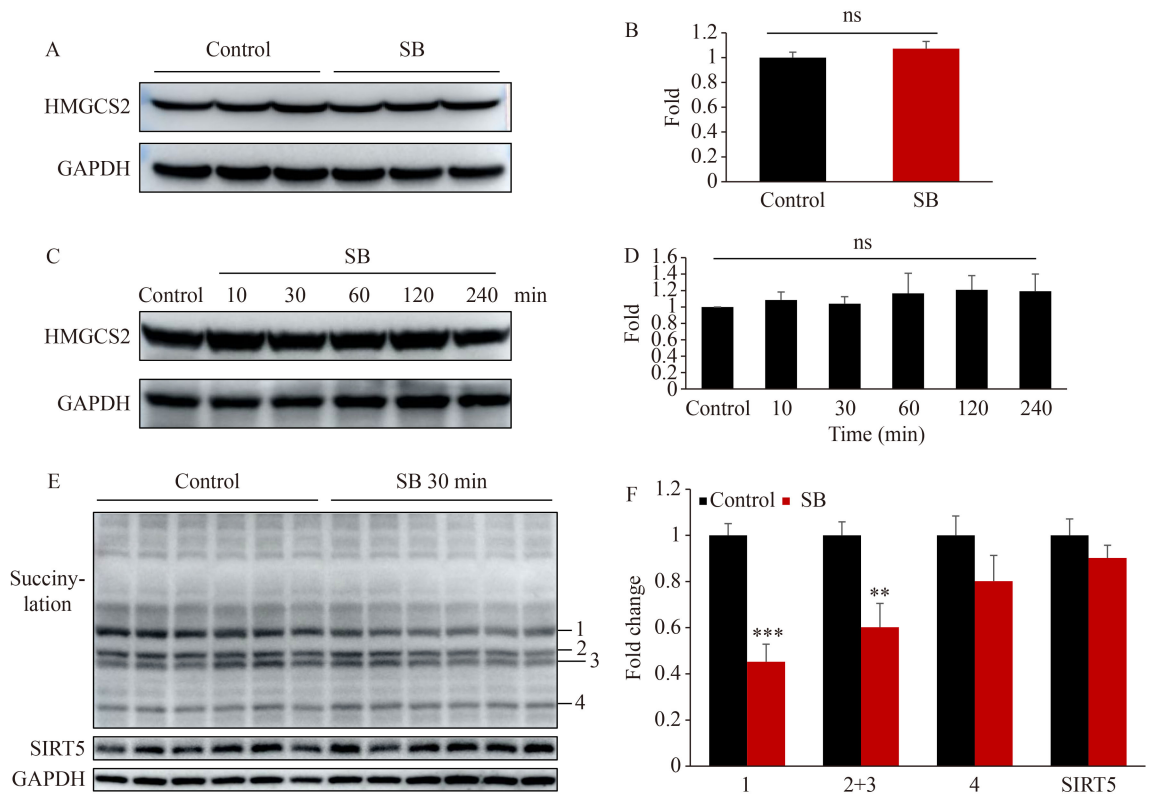

Fig. 4 SB has no effect on the protein level of HMGCS2. (A,B) HMGCS2 protein in the liver tissue determined by Western blot ($n = 3$). (C,D) The protein level of HMGCS2 in the liver at 5 time points of SB treatment in Western blot ($n = 4$). (E,F) Protein succinylation and SIRT5 protein in the liver tissue at 30 min after SB injection in Western blot. SB was administrated at 2.5 g/kg by intraperitoneal injection. ** $P < 0.01$, ***$P < 0.001$.

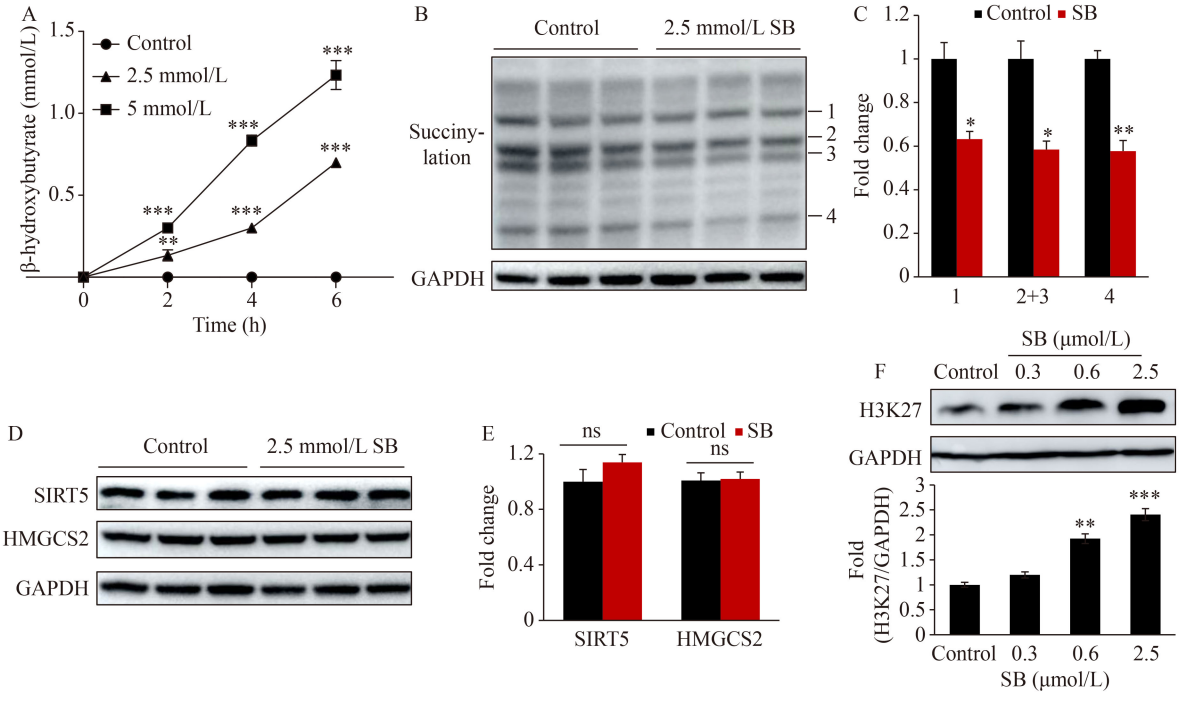

Fig. 5 SB promotes ketogenesis in primary hepatocytes and reduces the level of succinylation. (A) BHB production by the primary hepatocytes. BHB in the cell supernatant was detected with the BHB meter at different dosages and time points of SB treatment ($n = 3$). (B,C) Protein succinylation profile in the primary hepatocytes after SB treatment. (D,E) The protein levels of SIRT5 and HMGCS2 determined by Western blot. (F) Histone acetylation at H3K27 in the liver tissue of SB-treated mice as an indicator of HDAC inhibition. * $P < 0.05$, ** $P < 0.01$, *** $P < 0.001$.

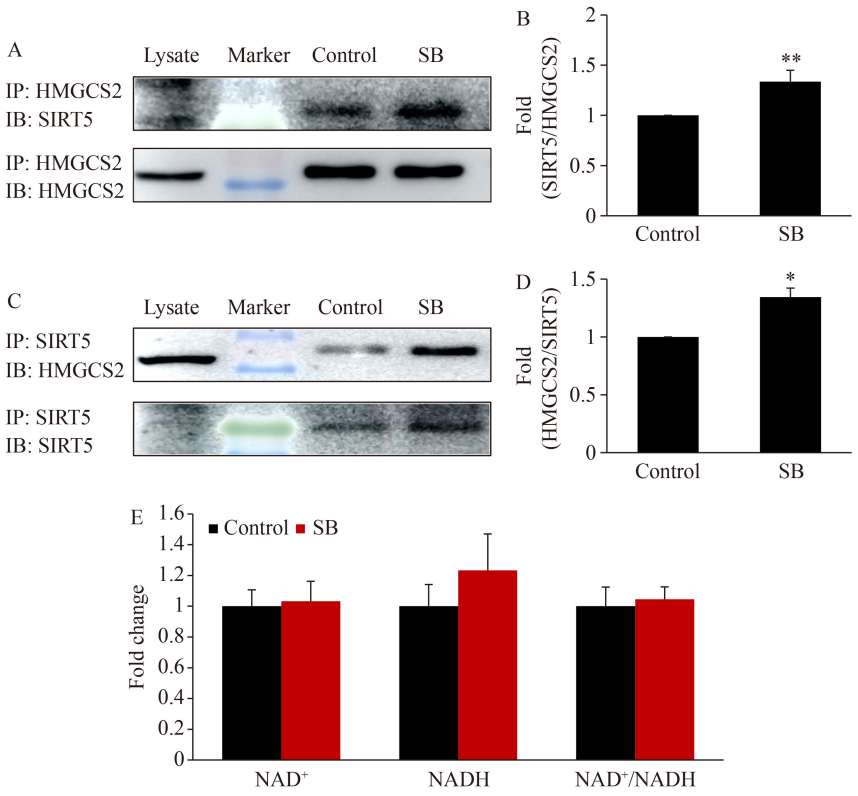

Fig. 6 SB increases the interaction between HMGCS2 and SIRT5. IP was conducted in the homogenate of liver tissues that were obtained at 0.5 h of SB (2.5 g/kg) intraperitoneal injection. (A,B) HMGCS2 and SIRT5 interaction was investigated in the IP products of HMGCS2 (n = 4). (C,D) HMGCS2 and SIRT5 interaction was studied in the IP products of SIRT5 (n = 3). (E) Levels of NAD^+ and NADH and their ratio in the liver tissue at 0.5 h of SB injection. NAD^+ and NADH were detected with LC/MS (n = 6). * $P < 0.05$, ** $P < 0.01$.

mice, as indicated by the fall in plasma BHB under the fasting state (Fig. 7G). In response to SB, the plasma BHB elevation was significantly reduced in Sirt5-KO mice in the first hour, but the difference was lost at 2 h and thereafter (Fig. 7H). When the hepatocytes of Sirt5-KO mice were examined in the cell culture, SB-induced ketogenesis was decreased even at 4 h of SB treatment (Fig. 7I). These observations suggest that SIRT5 may be required for the SB effect on hepatocytes in the ketone body production. However, a SIRT5-independent mechanism may mediate the SB activity *in vivo* as well because the difference of KO and WT mice in ketone body disappeared after 2 h of SB challenge.

Discussion

Our data suggests that SB regulates protein succinylation in hepatocyte mitochondria in the control of ketone body production. Mitochondrial functions are extensively regulated by post-translational protein modifications, such as acetylation and succinylation [23]. The modifications are induced by metabolic substrates and products for quick and accurate responses to the changes in cellular environment, which are critical in the maintenance of energy homeostasis. However, the mitochondrial response to SB remains largely unknown, except for the elevation in protein acetylation [11]. Succinylation was investigated in mitochondrial proteins in the mechanism of SB induction of ketone body production.

The screening approach of targeted proteomics reveals that HMGCS2 succinylation was downregulated by SB. It has been known for a long time that butyrate can be converted into BHB through activation of the rate-limiting enzyme HMGCS2 [24]. However, the molecular mechanism remains unknown for the SB activity. Lysine is a residue for diverse modification, including acetylation, succinylation, malonylation, glutarylation, crotonylation, and betahydroxyisobutyrylation [25]. SB activity in the induction of acetylation has been well-known, but its activity in the regulation of succinylation has been unknown [26]. We screened proteins for succinylation with targeted proteomics approach and found that more than 900 proteins were succinylated in the mouse liver. The succinylation pattern was modified by SB, and the most significant effect was observed on the mitochondrial proteins, which accounted for 41.4% in the downregulated proteins and 65.4% in the upregulated proteins. The catalytic activity of HMGCS2 is induced by the desuccinylation of K83 and K310 in a published study

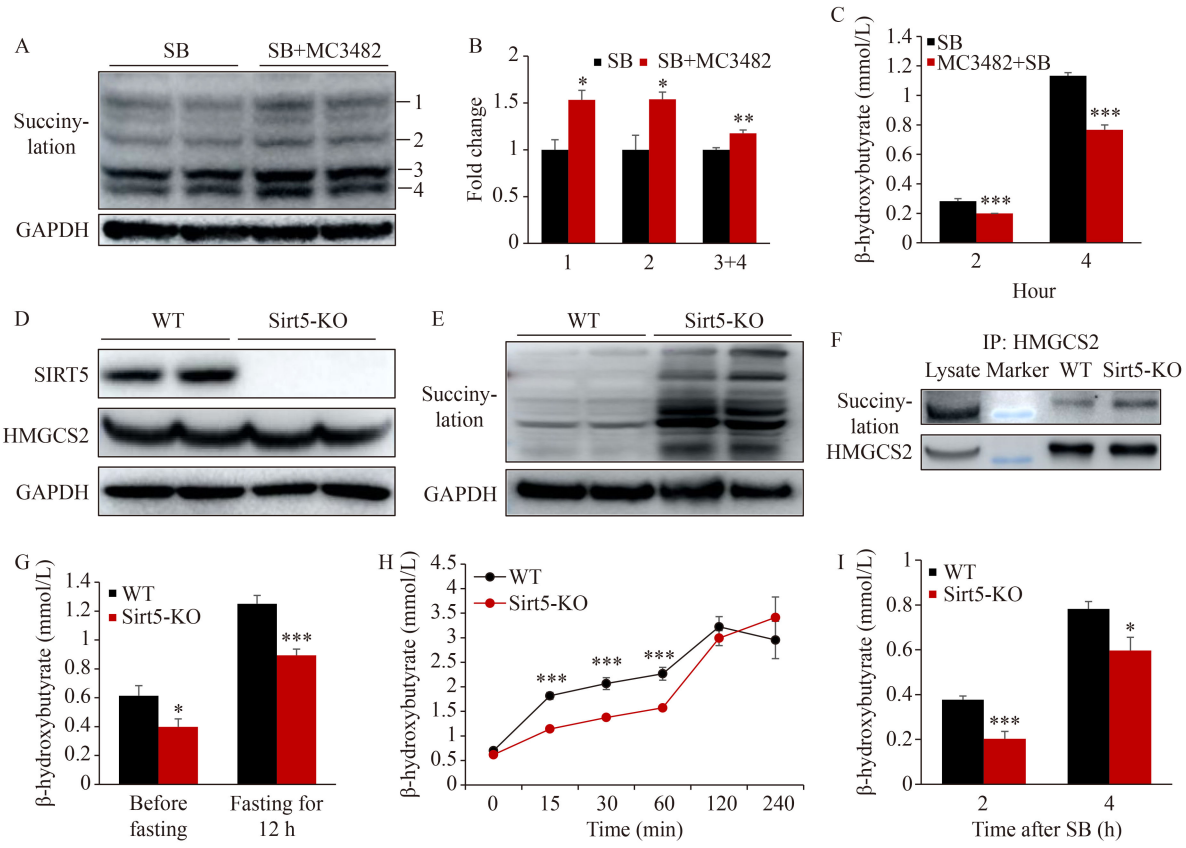

Fig. 7 SIRT5 plays an important role in ketogenesis of SB. (A) Protein succinylation of primary hepatocytes of C57BL/6 mice in the presence of SIRT5 inhibitor MC3482. The cells were pretreated with MC3482 (100 μmol/L) for 1 h before the SB (2.5 mmol/L) treatment. (B) Quantification of A (n = 4). (C) BHB in the supernatant of primary hepatocytes treated with MC3482 and SB (2.5 mmol/L) (n = 6). (D) SIRT5 and HMGCS2 proteins in the liver of Sirt5-KO mice. (E) Protein succinylation in the liver of Sirt5-KO mice. (F) Succinylation of HMGCS2 protein in the liver of Sirt5-KO mice in the IP study. (G) Blood ketone body levels in the Sirt5-KO mice in the fasting and non-fasting conditions (WT, n = 7; Sirt5-KO, n = 6). (H) Blood BHB levels in Sirt5-KO mice with SB challenge (2.5 g/kg, i.p.) for 4 h (n = 6). (I) BHB in the supernatant of primary hepatocytes of Sirt5-KO mice (n = 6). * $P < 0.05$, ** $P < 0.01$, *** $P < 0.001$.

on SIRT5 activity [21]. In this study, succinylation of the two lysine residues were not altered by SB during induction of catalytic activity of HMGCS2. Instead, the desuccinylation at K221 and K358 was induced by SB for activation of HMGCS2, which have not been reported in the literature. Both succinylation and acetylation were detected at K221, but K221 acetylation was not increased by SB. This result does not support the possibility of competition between the two modifications at the same lysin residue. HMGCS2 protein acetylation was induced by SB at K243 and K310 in the proteomics data. Significance of the acetylation alteration remains unknown for HMGCS2 enzyme. The data of SIRT5 inhibitor and Sirt5-KO mice suggests that SB induced the catalytic activity of HMGCS2 through the desuccinylation of the two lysine residues, namely, K221 and K358.

Current study suggests that SB may activate SIRT5 through a novel NAD^+ independent pathway. The SB effect was dependent on SIRT5, as shown by the data from the SIRT5 inhibitor and Sirt5-KO mice. The SB induced interaction of HMGCS2 and SIRT5 in desuccinylation in this study, which suggests that SB may activate SIRT5. To understand the mechanism of SB activity, we examined NAD^+/NADH ratio in the liver of SB-treated mice with targeted metabolomics. SIRT5 belongs to the sirtuin family, which are NAD^+-dependent deacetylases, including SIRT1–SIRT7 [27]. The catalytic activity of SIRT5 is induced by the elevation of NAD^+ [22]. SIRT5 exists in the mitochondria and is the only enzyme that is currently known for desuccinylation [26]. Recent studies identified α-ketoglutarate dehydrogenase (OGDH) and carnitine palmitoyl transferase 1A (CPT1A) as succinyltransferases [28,29]. The metabolomics data suggests that NAD^+/NADH ratio was not altered in the liver by SB, suggesting that SIRT5 might be activated by an unknown mechanism. The SIRT5 activity is modified by protein acetylation. However, no significant change was detected in the acetylation and succinylation of SIRT5 protein in the liver of SB-treated mice in the current study (Table S1). The SIRT5 activation by SB may represent a new SB activity in the regulation of protein modification.

In addition to succinylation, acetylation also regulates HMGCS2 activity [30]. In Shimazu's study, SIRT3 promoted ketone body production during fasting by reducing HMGCS2 acetylation [30]. However, acetylation was elevated in the current study at two sites in HMGCS2 protein, including K243 and K310 in the SB-treated group, which was associated with the elevated HMGCS2 activity. The acetylation effect was opposite to that reported in Shimazu's study. Our data could not exclude the role of acetylation in the regulation of HMGCS2 activity. Acetylation may mediate a part of SB activity in the induction of HMGCS2 activity, such as the induction of conformation change in the HMGCS2 protein in favor of interaction with SIRT5. The acetylation effect on HMGCS2 needs further investigation.

In summary, our data suggest that SB regulates protein succinylation in the control of liver metabolism. This point is supported by the SB induction of HMGCS2 desuccinylation in the liver ketogenesis model. SIRT5 may mediate SB signal in the desuccinylation of HMGCS2. Our data suggests that SIRT5 activation by SB may not require an elevation in NAD^+ level. The mechanism of SB induction of ketogenesis is dependent on HMGCS2/SIRT5 interaction. The data suggest that SIRT5 may act on K221 and K358 in the HMGCS2 protein for desuccinylation. This possibility deserves to be tested in more sophisticated experiments, such as point mutation of HMGCS2, identification of interaction domains of SIRT5 and HMGCS2, and rescue of Sirt5-KO hepatocytes with modified HMGCS2.

Acknowledgements

The project was supported by the National Key Research and Development Program of China (No. 2018YFA0800603) and a project (No. 19ZR1439000) of the Shanghai Association for Science and Technology to Jianping Ye.

Compliance with ethics guidelines

Yanhong Xu, Xiaotong Ye, Yang Zhou, Xinyu Cao, Shiqiao Peng, Yue Peng, Xiaoying Zhang, Yili Sun, Haowen Jiang, Wenying Huang, Hongkai Lian, Jiajun Yang, Jia Li, and Jianping Ye declare that they have no conflict of interest. All institutional and national guidelines for the care and use of laboratory animals were followed.

Electronic Supplementary Material Supplementary material is available in the online version of this article at https://doi.org/10.1007/s11684-022-0943-0 and is accessible for authorized users.

References

1. Dhatariya KK, Glaser NS, Codner E, Umpierrez GE. Diabetic ketoacidosis. Nat Rev Dis Primers 2020; 6(1): 40
2. Veech RL, Bradshaw PC, Clarke K, Curtis W, Pawlosky R, King MT. Ketone bodies mimic the life span extending properties of caloric restriction. IUBMB Life 2017; 69(5): 305–314
3. Sedej S. Ketone bodies to the rescue for an aging heart? Cardiovasc Res 2018; 114(1): e1–e2
4. Hernandez AR, Hernandez CM, Campos KT, Truckenbrod LM, Sakarya Y, McQuail Ph DJ, Carter CS, Bizon JL, Maurer AP, Burke SN. The anti-epileptic ketogenic diet alters hippocampal transporter levels and reduces adiposity in aged rats. J Gerontol A Biol Sci Med Sci 2018; 73(4): 450–458
5. Shippy DC, Wilhelm C, Viharkumar PA, Raife TJ, Ulland TK. β-Hydroxybutyrate inhibits inflammasome activation to attenuate Alzheimer's disease pathology. J Neuroinflammation 2020; 17(1): 280
6. Harvey CJDC, Schofield GM, Williden M. The use of nutritional supplements to induce ketosis and reduce symptoms associated with keto-induction: a narrative review. PeerJ 2018; 6: e4488
7. Gao Z, Yin J, Zhang J, Ward RE, Martin RJ, Lefevre M, Cefalu WT, Ye J. Butyrate improves insulin sensitivity and increases energy expenditure in mice. Diabetes 2009; 58(7): 1509–1517
8. Mollica MP, Mattace Raso G, Cavaliere G, Trinchese G, De Filippo C, Aceto S, Prisco M, Pirozzi C, Di Guida F, Lama A, Crispino M, Tronino D, Di Vaio P, Berni Canani R, Calignano A, Meli R. Butyrate regulates liver mitochondrial function, efficiency, and dynamics in insulin-resistant obese mice. Diabetes 2017; 66(5): 1405–1418
9. Parada Venegas D, De la Fuente MK, Landskron G, González MJ, Quera R, Dijkstra G, Harmsen HJM, Faber KN, Hermoso MA. Short chain fatty acids (SCFAs)-mediated gut epithelial and immune regulation and its relevance for inflammatory bowel diseases. Front Immunol 2019; 10: 277
10. McNabney SM, Henagan TM. Short chain fatty acids in the colon and peripheral tissues: a focus on butyrate, colon cancer, obesity and insulin resistance. Nutrients 2017; 9(12): 1348
11. Stilling RM, van de Wouw M, Clarke G, Stanton C, Dinan TG, Cryan JF. The neuropharmacology of butyrate: the bread and butter of the microbiota-gut-brain axis? Neurochem Int 2016; 99: 110–132
12. Vicente F, Rodríguez ML, Martínez-Fernández A, Soldado A, Argamentería A, Peláez M, de la Roza-Delgado B. Subclinical ketosis on dairy cows in transition period in farms with contrasting butyric acid contents in silages. ScientificWorldJournal 2014; 2014: 279614
13. Herrick KJ, Hippen AR, Kalscheur KF, Schingoethe DJ, Casper DP, Moreland SC, van Eys JE. Single-dose infusion of sodium butyrate, but not lactose, increases plasma β-hydroxybutyrate and insulin in lactating dairy cows. J Dairy Sci 2017; 100(1): 757–768
14. Xu Y, Peng S, Cao X, Qian S, Shen S, Luo J, Zhang X, Sun H, Shen WL, Jia W, Ye J. High doses of butyrate induce a reversible body temperature drop through transient proton leak in mitochondria of brain neurons. Life Sci 2021; 278: 119614
15. Zhang Y, Sun Z, Jia J, Du T, Zhang N, Tang Y, Fang Y, Fang D. Overview of histone modification. Adv Exp Med Biol 2021; 1283: 1–16
16. Liu H, Wang J, He T, Becker S, Zhang G, Li D, Ma X. Butyrate: a double-edged sword for health? Adv Nutr 2018; 9(1): 21–29
17. Kulkarni SS, Cantó C. Mitochondrial post-translational

modifications and metabolic control: sirtuins and beyond. Curr Diabetes Rev 2017; 13(4): 338–351
18. Stram AR, Payne RM. Post-translational modifications in mitochondria: protein signaling in the powerhouse. Cell Mol Life Sci 2016; 73(21): 4063–4073
19. Cao X, Ye X, Zhang S, Wang L, Xu Y, Peng S, Zhou Y, Peng Y, Li J, Zhang X, Han X, Huang WY, Jia W, Ye J. ADP induces blood glucose through direct and indirect mechanisms in promotion of hepatic gluconeogenesis by elevation of NADH. Front Endocrinol (Lausanne) 2021; 12: 663530
20. Nanchen A, Fuhrer T, Sauer U. Determination of metabolic flux ratios from ^{13}C-experiments and gas chromatography-mass spectrometry data: protocol and principles. Methods Mol Biol 2007; 358: 177–197
21. Rardin MJ, He W, Nishida Y, Newman JC, Carrico C, Danielson SR, Guo A, Gut P, Sahu AK, Li B, Uppala R, Fitch M, Riiff T, Zhu L, Zhou J, Mulhern D, Stevens RD, Ilkayeva OR, Newgard CB, Jacobson MP, Hellerstein M, Goetzman ES, Gibson BW, Verdin E. SIRT5 regulates the mitochondrial lysine succinylome and metabolic networks. Cell Metab 2013; 18(6): 920–933
22. Du J, Zhou Y, Su X, Yu JJ, Khan S, Jiang H, Kim J, Woo J, Kim JH, Choi BH, He B, Chen W, Zhang S, Cerione RA, Auwerx J, Hao Q, Lin H. Sirt5 is a NAD-dependent protein lysine demalonylase and desuccinylase. Science 2011; 334(6057): 806–809
23. Hofer A, Wenz T. Post-translational modification of mitochondria as a novel mode of regulation. Exp Gerontol 2014; 56: 202–220
24. Henning SJ, Hird FJ. Ketogenesis from butyrate and acetate by the caecum and the colon of rabbits. Biochem J 1972; 130(3): 785–790
25. Sabari BR, Zhang D, Allis CD, Zhao Y. Metabolic regulation of gene expression through histone acylations. Nat Rev Mol Cell Biol 2017; 18(2): 90–101
26. Park J, Chen Y, Tishkoff DX, Peng C, Tan M, Dai L, Xie Z, Zhang Y, Zwaans BM, Skinner ME, Lombard DB, Zhao Y. SIRT5-mediated lysine desuccinylation impacts diverse metabolic pathways. Mol Cell 2013; 50(6): 919–930
27. Carafa V, Rotili D, Forgione M, Cuomo F, Serretiello E, Hailu GS, Jarho E, Lahtela-Kakkonen M, Mai A, Altucci L. Sirtuin functions and modulation: from chemistry to the clinic. Clin Epigenetics 2016; 8(1): 61
28. Wang Y, Guo YR, Liu K, Yin Z, Liu R, Xia Y, Tan L, Yang P, Lee JH, Li XJ, Hawke D, Zheng Y, Qian X, Lyu J, He J, Xing D, Tao YJ, Lu Z. KAT2A coupled with the α-KGDH complex acts as a histone H3 succinyltransferase. Nature 2017; 552(7684): 273–277
29. Kurmi K, Hitosugi S, Wiese EK, Boakye-Agyeman F, Gonsalves WI, Lou Z, Karnitz LM, Goetz MP, Hitosugi T. Carnitine palmitoyltransferase 1A has a lysine succinyltransferase activity. Cell Rep 2018; 22(6): 1365–1373
30. Shimazu T, Hirschey MD, Hua L, Dittenhafer-Reed KE, Schwer B, Lombard DB, Li Y, Bunkenborg J, Alt FW, Denu JM, Jacobson MP, Verdin E. SIRT3 deacetylates mitochondrial 3-hydroxy-3-methylglutaryl CoA synthase 2 and regulates ketone body production. Cell Metab 2010; 12(6): 654–661